Available online at www.sciencedirect.com
SCIENCE DIRECT®
Marine Geology 199 (2003) 181–204
MARINE GEOLOGY
INTERNATIONAL JOURNAL OF MARINE GEOLOGY, GEOCHEMISTRY AND GEOPHYSICS
www.elsevier.com/locate/margeo

Analysis and modelling of gravity- and piston coring based on soil mechanics

L.C. Skinner [a,*], I.N. McCave [b]

[a] Godwin Laboratory, Department of Earth Sciences, Cambridge University, Pembroke Street, New Museums Site, Cambridge CB2 2SA, UK
[b] Department of Earth Sciences, Cambridge University, Downing Street, Cambridge CB2 3EQ, UK

Received 24 June 2002; accepted 25 April 2003

Abstract

The effects of gravity- and piston corers on the dimensional accuracy of marine sediment cores is analysed using principles of soil mechanics. A model for the coring process is built around the feedback that arises and develops between the core barrel and the sampled sediment. This model for sediment response is applied to different hypothetical coring scenarios, which are then compared to real examples, providing insights into the specific effects of each sampling method and the development of these effects down-core. Four cores from a single location on the Iberian Margin are found to contain stratigraphically intact successions that differ in length by a factor of up to 2.7, due solely to the different effects of each coring method. These dimensional discrepancies are attributed to the combined effects of 'over-sampling' in the upper portions of the piston cores (due to cable rebound causing upward piston acceleration), and 'under-sampling' dominant in the basal portions of the open-barrel gravity-type cores. It is suggested that heavier piston corers, deployed on longer, lighter cables, are prone to greater over-sampling ratios over longer stratigraphic intervals, due to the increased likelihood and extent of cable rebound. Cable rebound may also give rise to double penetration of gravity corers, resulting in repeated stratigraphic intervals. Knowledge of the dimensional accuracy of marine sediment cores is essential to an evaluation of past sedimentation rates, and hence interpretations of past depositional processes. It is therefore essential that we recognise the sampling effects of each coring method, and their variability down-core, lest coring artefacts be interpreted as sedimentary signals. Different core types may be more suited to different palaeoceanographic investigations. Hence, failing the development of a practical cable-deployed recoilless piston corer, a combination of a variety of core types will permit the best acquisition of the in situ stratigraphic truth. Our results suggest that a large-diameter ($D_c \sim 20$–30 cm) square-barrel gravity corer for the top 10–12 m combined with a cylindrical piston corer below ~ 10 m may provide the least deformed material.

Keywords: coring; soil mechanics; piston; IMAGES; Calypso; Kasten

1. Introduction

Marine sediments provide us with essential records of palaeoenvironments, offering the

* Corresponding author. Fax: +44-1223-334-871.
E-mail address: luke00@esc.cam.ac.uk (L.C. Skinner).

0025-3227/03/$ – see front matter © 2003 Elsevier Science B.V. All rights reserved.
doi:10.1016/S0025-3227(03)00127-0

length, continuity and resolution that continental records rarely afford. A proper interpretation of marine sediment cores, however, requires us to distinguish 'primary' stratigraphic features from 'secondary' artefacts that are almost inevitably introduced during the sampling process. For the purposes of palaeoenvironmental studies it is desirable to preserve the sediment column's in situ structure and dimensions. Preservation of structure and microfabric bears on the stratigraphic integrity and resolution of the record. Preservation of dimensions is essential for inference of mass flux, and hence depositional processes.

The challenge of accessing the wealth of information recorded in marine sediments has been met with an arsenal of coring techniques, of which the piston corer represented a major advance (Kullenberg, 1947, 1955). Inevitably, every sampling technique affects the sedimentary column in a particular manner, potentially introducing dimensional and structural changes. An evaluation of the effects of each coring technique on the resulting sediment core is therefore essential. Emery and Dietz (1941) noted that many open-barrel gravity cores they obtained were shorter than the length of corer penetration (indicated by a mud line on the core barrel), suggesting up to 50% 'shortening' of the retrieved sediment column. Lebel et al. (1982) confirmed these findings through a comparison of pore-water chemical gradients obtained from cylindrical gravity cores and 'virtually undisturbed' box cores (up to 1 m long) retrieved from the same locations. Their suggestion was that although gravity core shortening varied from location to location, it was essentially linear throughout each individual core. This interpretation was challenged by Parker and Sills (1990) and Parker (1991), who indicate that during the coring process 'entry deficits' (penetration minus sample entry) may develop continuously *or* intermittently, producing positive deficits due to impeded entry or negative deficits due to internal suction or expansion. Furthermore, they suggested that cylindrical gravity corers are more susceptible to developing entry deficits than are square 'Kasten'-type corers (Parker and Sills, 1990). Hence the specific effects of a given corer are uniquely determined by the highly variable interactions between its dimensions/construction and the sediment characteristics (Blomquist, 1985), as they develop throughout the coring process.

Although detailed studies of piston core entry deficits have not been undertaken, photographic analysis of piston core sampling has revealed that these too are subject to extremely variable behaviour (McCoy, 1980). Indeed, comparisons of simultaneously recovered piston- and gravity cores have illustrated that at times the piston cores may be shortened relative to the gravity cores, while in other cases the opposite may be true (e.g. Ericson and Wollin, 1956; Emery and Hulsemann, 1964; Ross and Riedel, 1967). In these comparisons, reduced lengths of gravity cores were attributed to sediment 'thinning', while shortening of piston cores was attributed to the loss of core-top material 'smeared' down the core barrel as well as sediment thinning at intermediate depths. Hence, it has been generally assumed that all deformation tends to condense the stratigraphy, or be 'destructive'.

Although this may be a sound assumption for gravity-type corers, it may not necessarily remain valid for piston corers, in which relative motion between the sediment core and the piston during recovery may result in negative relative pressures inside the core barrel above the sediment being sampled. The frequent occurrence of collapsed piston core liners is clear evidence of such a phenomenon (e.g. Bassinot and Labeyrie, 1996). Furthermore, it has been noted that under-pressuring of the piston corer during entry may produce 'flow-in' (Bouma and Boerma, 1968; McCoy, 1985), giving rise to vertical disturbances and destroying stratigraphic integrity in extreme cases. This has been noted most often at the *base* of piston cores, but it may also occur mid-core and may go unnoticed if the effect has been too subdued to destroy the visible primary sedimentary fabric. Indeed, Buckley et al. (1994) have shown that flow-in may occur variably throughout a single piston core, as may its stratigraphically 'destructive' opposite, which they refer to as 'sediment by-passing'. Mid-core flow-in, or 'oversampling', was generally associated with upward

accelerations in the lowering cable and subsequent changes in the core-liner cavity pressure, suggesting elastic 'recoil' of the cable as the cause of the problem. Sediment by-passing, however, was usually limited to the basal portions of the piston cores, as a result of sediment 'binding' or 'plugging' when the weight of the corer came to equal the end-bearing capacity and the frictional resistance of the sediments, stopping the corer as a result.

In order to address the issue of dimensional artefacts in marine sediment cores, more complex cable-deployed corer designs have been proposed (Weaver and Schultheiss, 1990), beginning with the Giant Piston Corer (Hollister et al., 1973; Driscoll and Hollister, 1974) and its improved successor the Advanced Piston Corer (APC) (Silva et al., 1976; Weaver and Schultheiss, 1990). Although initially successful, the relative complexity and impracticality of these corer designs appears to have hindered their widespread usage by the palaeoceanographic community. The same might be said of the STACOR (stationary piston corer), developed by the Institut Francais du Petrole, Elf Aquitaine and Total (Montargues et al., 1983, 1987), which makes use of a mechanical pulley system to maintain the piston immobile and level with a fixed base-plate that rests on the sediment–water interface outside the core barrel. Although this device yields sediment cores of excellent quality and dimensional integrity it suffers, like the APC, from major practical drawbacks, not least its particularly time-consuming deployment.

Perhaps the most successful design of recoilless piston corer is the APC of the Ocean Drilling Program (ODP-APC) (Storms, 1990). Unlike the cable-deployed devices, the ODP-APC is deployed from a rigid drill pipe surmounted by a heave compensator to eliminate drill-string motion and uses hydraulic pressuring to 'fire' the core barrel into the sediment, past a stationary piston. Although very successful, this corer design is highly specialised, requiring a drilling vessel for its deployment. Hence the cable-deployed Kullenberg-type piston corer remains the most practical and widely used coring device for obtaining deep-sea sediment cores that sample the mid- to late Pleistocene. The Calypso corer, designed by Yvon Balut (IFRTP), is a successful example of such a device, permitting the recovery of very long cores without requiring particularly sophisticated or expensive technology. The fact that corers such as the Calypso remain so much more practical and widely used in palaeoceanographic studies than the more complex designs of 'recoilless' piston corers makes a critical analysis of their effects on marine sediment samples essential.

This paper analyses the effects of cable-deployed gravity- and simple Kullenberg-type piston corers (such as the Calypso) on the dimensional accuracy of marine sediment samples by drawing on principles of soil mechanics. A conceptual model for the coring process is built around the feedback that arises and develops incrementally between the penetrating core barrel and the sampled sediment. This 'model' for sediment response is applied to different hypothetical coring scenarios, which are then compared to real examples.

2. Theory and analysis of coring

2.1. 'Tube sampling': cumulative friction

An element of soil being sampled deforms by virtue of changes in the stress applied to it. Fig. 1A illustrates a soil element inside an open-ended tube, analogous to a pistonless core barrel or gravity corer. Between this soil element and the core-barrel walls, a frictional force is generated as the corer descends past it. It can be shown that the rapidity with which the corer descends (requiring only a few seconds), and the very low permeability of clayey fine-grained marine sediments (10^{-14}–10^{-16} m^2), precludes the flow of pore water. The only potential for true compaction or dilation of the sampled sediments occurs well after the retrieval of the core. Hence 'undrained' conditions prevail and the friction between the sediment and the core barrel may be related to the undrained shear strength of the soil element (C_{ui}), the total contact area between the soil element and the corer (A_{si}), and a 'skin friction' factor (α).

The skin friction factor accounts for the relative ease of sediment sliding past the steel barrel or plastic liner, as compared to sediment–sediment shearing (Meyerhof, 1976). Although the skin friction factor is notoriously difficult to constrain, a value of ~0.3–0.5 is commonly used for soft saturated clays (Meyerhof, 1976; Smith and Smith, 1998) (a value of 0.35 is adopted here). Furthermore, from X-radiographs and direct observations of marine cores, it appears that a significant amount of the friction between the sediment and the core barrel may be attenuated by 'smearing' and/or the development of a mud slick along the sediment–corer interface. The skin friction factor (α) is therefore likely to be quite low and may vary along the core, increasing downwards to a maximum near the core base. Hence, for a thin soil element (labelled i), at depth z, of inner wall contact area $\mathrm{d}A_{si}$ and shear strength C_{ui}, the frictional force between it and the core barrel ($\mathrm{d}F_i$) may be expressed as:

$$\mathrm{d}F_i = \alpha C_{ui} \mathrm{d}A_{si} \quad (1)$$

As the corer descends, more increments of soil enter the barrel (Fig. 1B), and each of them supplies an additional increment of frictional force, directed downwards. Summing across the entire length of sediment sampled yields a net vertical stress (above lithostatic) under the core nose:

$$\Delta\sigma_{vz} = \sum_{i=0}^{z} \frac{\alpha C_{ui} \mathrm{d}A_{si}}{A_x} \quad (2)$$

where A_x is the inner cross-sectional area of the core nose. For both square and cylindrical core barrels of diameter (or side-length) D_c, and a soil element of thickness $\mathrm{d}z_i$, the ratio of inner contact area to cross-sectional area is:

$$\frac{\mathrm{d}A_{si}}{A_x} = \left(\frac{4\mathrm{d}z_i \pi D_c}{\pi D_c^2}\right)_{\text{round}} \equiv \left(\frac{4\mathrm{d}z_i D_c}{D_c^2}\right)_{\text{square}} = \frac{4\mathrm{d}z_i}{D_c} \quad (3)$$

Hence, substituting Eq. 3 into Eq. 2, for both square and cylindrical core barrels:

$$\Delta\sigma_{vz} = \frac{4\alpha}{D_c} \sum_{i=0}^{z} C_{ui} \mathrm{d}z_i \quad (4)$$

As the corer descends further it exerts an increasing vertical stress on the sediments below it (i.e. on the sediments about to be sampled). This is due to: (i) the increasing total soil–barrel internal contact area (A_s); and (ii) a general increase in undrained shear strength (C_{ui}) with increasing sediment depth (i.e. as i increases in Eq. 4). There is also some upward friction on the barrel due to the external soil–barrel contact area, which we ignore here. Although the undrained shear strength of marine mud clearly cannot increase monotonically to infinity, shear vane measurements suggest that it does increase approximately linearly with depth from a minimum of approximately 1 kPa at the sediment–water interface, to ~20 kPa at 15 m sediment depth (Silva et al., 1976; Silva and Hollister, 1979). Hence, for sediment penetration depths not exceeding ~30–40 m, and ignoring specific effects of small-scale variations in lithology ($CaCO_3$ content in particular affects the detail of C_u trends), $C_u(z)$ may adequately be given by:

$$C_u(z) = 1 + 1.3z \text{ (in kPa for } z \text{ in m)} \quad (5)$$

Hence, in general a descending core barrel accumulates an increasing sediment column inside it, which is subjected to an increasing downward frictional drag. This friction is transferred through the soil column (pore-fluid flow is too slow to dissipate it) and is imposed over the cross-sectional area of the core aperture as a vertical stress on the soil immediately below the corer at that instant in its descent. Geotechnical studies of hollow piles driven into unconsolidated saturated soils (which provide a direct analogy with tube sampling and have been studied extensively in the engineering literature) indicate that vertical stresses within a soil column inside a pile reach a maximum near its base and decrease rapidly up the soil column (Paik and Lee, 1993). In this way, soil higher up in the tube essentially does not contribute to the cumulative frictional stress at the base. An analogous situation is assumed here for tube sampling, though it is attributed to the development of 'sediment smearing' at the core margins. This causes less side-wall friction to be transferred to the core base as a vertical pressure, contributing to localised strain instead (see Fig. 1C). Hence we model σ_{vz} by summing the friction contributions over only the basal

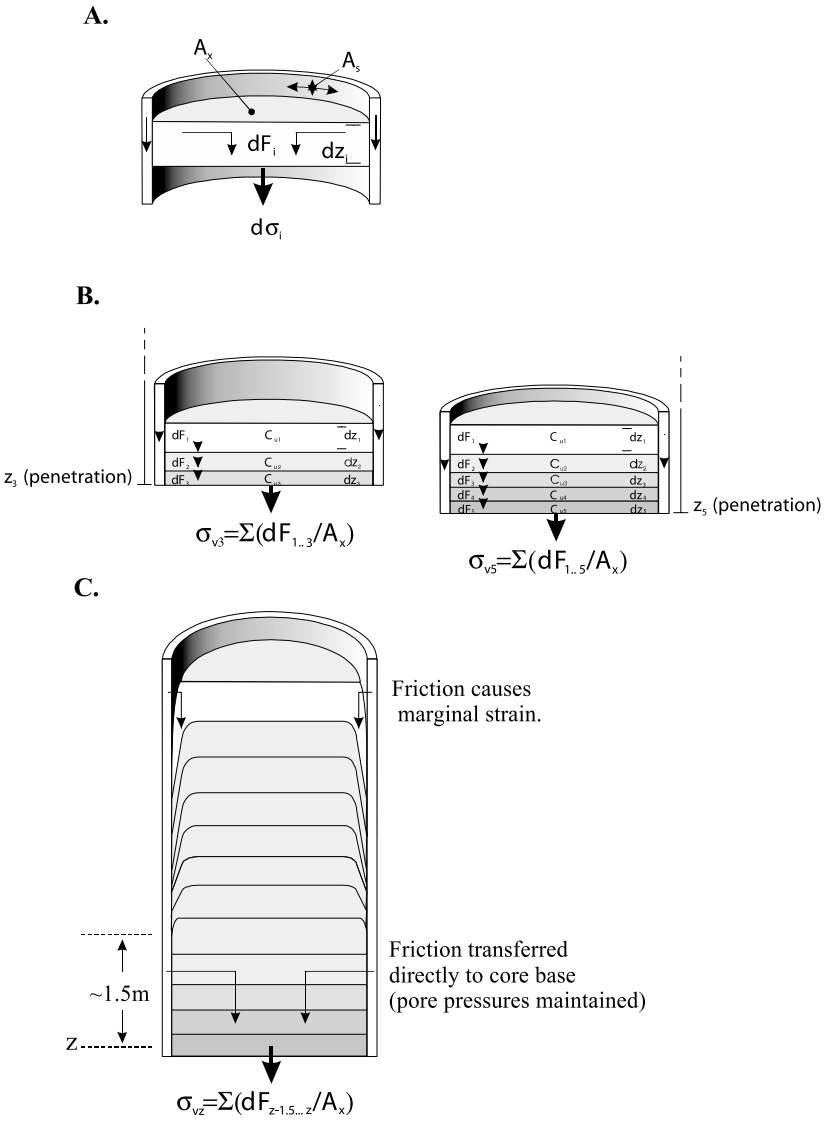

Fig. 1. (A) Each increment of soil entering the core barrel contributes an increment of friction (dF_i) that depends on the thickness of the soil increment (dz_i), its shear strength and the skin-friction factor between soil and corer. The friction is applied across the cross-sectional area of the corer as a vertical stress ($d\sigma_i$) imposed on the soil about to be sampled. (B) Successive soil elements entering the corer contribute to the cumulative friction and the resulting vertical stress beneath the corer. The friction provided by a given soil element will depend on its thickness, and the thickness of each soil element will depend on how it is affected by the vertical stress provided by the preceding soil elements. The shear strength (C_{ui}) will increase approximately linearly with sediment depth, such that deeper soil elements will contribute more friction for a given thickness of sediment. The friction factor between soil and corer will also evolve with penetration. Soil–barrel interactions will therefore develop with increasing penetration, depending on an evolving balance between soil character and soil deformation. (C) A decrease in friction between soil and corer toward the top of the core barrel may result from the smearing of marginal sediment. Friction will cause local deformation rather than being transferred to the core base as a vertical pressure. Lower 'ultimate' or 'mobilised' shear strengths, and the release of occluded pore water to generate a mud slick or slurry, will also contribute to this effect, which renders the increase in cumulative friction with depth more linear.

~1.5 m of the sediment column (following de Nicola and Randolph (1997)), giving:

$$\Delta\sigma_{vz} = \frac{4\alpha}{D_c} \sum_{i=(z-1.5)}^{z} C_{ui} dz_i \quad (6)$$

The smearing of sediments at the core margins reduces side-wall friction by:

(i) allowing relative movement between the corer and the sediment;

(ii) producing a non-linear decrease in the sediment shear strength (to ultimate or 'mobilised' shear strengths); and

(iii) re-organising sediment particles, releasing occluded pore water and producing a lubricating slurry as a result.

These three effects combine to limit the contribution of friction up-core.

2.2. Sediment response, and entry

For a soil element on the descent trajectory of the corer, the vertical stress it experiences gradually increases from lithostatic equilibrium to a maximum just before it is 'captured' by the descending corer. Deeper soil elements experience greater maximum vertical stresses, since at greater depth the corer has accumulated more sediment of increasing shear strength, supplying more frictional drag. In response to the imposed maximum vertical stress, just before it is sampled, a given soil element will either remain essentially unaffected or yield to some extent. This may range from slight deformation to complete 'failure' by flow (it will not be compressed, as this requires pore-water displacement). In geotechnical applications, the transition from negligible or moderate deformation to complete failure is understood as a transition from 'unimpeded' to 'impeded' entry ('sediment by-passing'). In geotechnical engineering applications, 'piles' descending through unconsolidated sediments (i.e. hollow tubes analogous to corers) may exhibit three types of sediment entry: unplugged, partially plugged and fully plugged (e.g. de Nicola and Randolph, 1997; Randolph et al., 1991). These modes of soil entry are defined in terms of the 'incremental filling ratio' (IFR) of the tube, the ratio of an increment of undisturbed soil column length to the corresponding increment of tube penetration. Unplugged behaviour is characterised by the free movement of soil into the descending tube, corresponding to an IFR of 1, partially plugged behaviour by partially impeded soil entry (IFR between 0 and 1), and fully plugged behaviour by an IFR of 0.

IFRs greater than unity, representing greater soil entry than penetration, are also possible (due to soil expansion or soil over-sampling) and are indeed observed (e.g. Paik and Lee, 1993; Buckley et al., 1994). As shown above, during the sampling process the resistance to soil entry (provided by the soil–barrel friction inside the corer) gradually increases, and hence a general progression from unplugged, to partially plugged, to fully plugged behaviour is to be expected. Transitions from one entry mode to another, if they occur at all, are defined by the 'plug capacity' of the soil column inside the barrel. 'Plug capacity', in this context, may be understood as the balance between imposed vertical stress due to internal friction and in situ undrained bearing capacity (Q_{ub}) of the underlying sediments. The bearing capacity Q_{ub} represents the force that in situ sediments may support before failing completely, causing sediment by-passing. According to Meyerhof's (1951) equation, the bearing capacity pressure (C_b) for undrained saturated clayey sediments is given by:

$$C_b = \frac{Q_{ub}}{A_x} = N_c C_u \quad (7)$$

where N_c is a 'bearing capacity factor' generally accepted as equal to 9 for saturated undrained clayey sediments (Meyerhof, 1976). This analysis implies that when the imposed stress below the descending corer exceeds the shear strength of the underlying sediments by a factor of 9, then fully plugged behaviour will ensue. However, once the imposed 'frictional' stress reaches equilibrium with the in situ bearing pressure, they must *remain* in equilibrium. Hence, in principle, sediment actually continues to enter the corer in order to supply sufficient friction to balance any increase in bearing capacity due to increased penetration depth. The increment of soil (dL_z) entering the corer, as required in order to balance an

increase in bearing pressure (ΔC_b) due to further penetration (dz), depends on the length of soil column that contributes to the net vertical stress ($h = 1.5$, in Eq. 6). This is given by:

$$\Delta C_b = \frac{4\alpha}{D_c}(C_{uz}dL_z - C_{u(z-h)}dL_{u(z-h)})$$

giving:

$$dL_z = \frac{\Delta C_b D_c}{4\alpha C_{uz}} + \frac{dL_{(z-h)}\ C_{u(z-h)}}{C_{uz}} \quad (8)$$

where D_c is core diameter, $C_{u(z-h)}$ is undrained shear strength at depth $z-h$, and $dL_{(z-h)}$ is the increment of soil that entered at depth $z-h$. For uniform friction along the entire soil column, only the first term is needed. This process of incomplete soil entry, equated here with 'partially plugged' behaviour, represents the squeezing of soil into the sampling tube as frictional- and bearing pressures maintain equilibrium. Although this process is easily visualised as an alternation between plugged and unplugged behaviour, it might be more realistically seen as a continuous 'undersampling' or 'thinning' of the sediments when infinitesimal increments of penetration are considered (Lebel et al., 1982; Emery and Dietz, 1941). Incremental entry must actually vary at small scales due to fine-scale changes in shear strength resulting from lithological changes (e.g. carbonate or water content), though such fine-scale features are not considered here, and a linear depth–shear strength relation is assumed. A core barrel halts its descent when the mobilised end-bearing capacity of the sediments plus the mobilised inner and outer skin friction of the corer equals the immersed weight of the coring apparatus. Mobilised bearing capacities are generally lower than standing capacities (de Nicola and Randolph, 1997), hence re-mobilising a static soil column within a corer requires greater pressures than those required to maintain its continuous entry into the core barrel.

Fig. 2 illustrates the evolution of vertical imposed stress immediately below a descending tube sampler (i.e. gravity corer), arising from increasing internal friction which eventually balances increasing bearing capacity pressure below the transition depth labelled z_{crit}. Below z_{crit}, the preceding analysis (based on geotechnical pile-driving studies) suggests that in situ sediment responds to the descending corer by 'thinning' out under the imposed stress and being captured by the corer so as to maintain a balance between cumulative friction and bearing capacity pressures. This 'partially plugged' situation represents the transition between unplugged and fully plugged behaviour (as described above), and causes a significant 'condensation' of the stratigraphy being sampled. Above z_{crit}, however, unplugged entry allows sediments to enter the barrel while being subjected to an increased vertical stress. The sediments respond by sustaining a vertical strain, which may be approximated by an elastic solution of the type given by Poulos and Davies (1974). Differentiating the elastic solution for vertical displacement as a function of depth below cylindrical and square loads on an infinite elastic half-space, and solving for 15 cm square and 10 cm circular core barrels yields:

$$\varepsilon_{v\,max}(\text{square}) = \frac{-5.19\Delta\sigma_v}{\pi E} \quad (9)$$

$$\varepsilon_{v\,max}\ (\text{circle}) = \frac{-0.58\Delta\sigma_v}{E} \quad (10)$$

where $\varepsilon_{v\,max}$ is the maximum vertical strain below the load (occurring at a finite distance just below the load), E is the Young's modulus of the sediments (generally taken to be $\sim 300 C_u$) and $\Delta\sigma_v$ is the imposed stress due to corer–sediment friction, in excess of lithostatic pressure. These solutions demonstrate that the larger-diameter square sampling tube produces generally higher vertical strains than the narrower cylindrical tube for a given imposed load, though these 'elastic' strains are small compared to the shortening associated with partially plugged entry.

It is important to realise that marine sediments clearly are *not* elastic materials, and that what is being modelled as an elastic response is in fact a 'plastic flow' of essentially intact undrained sediment (i.e. with no change in porosity) (Weaver and Schultheiss, 1983). Hence, the response of a given stratigraphic 'element' to an imposed vertical stress is actually to 'thin' or 'thicken', rather than compacting or stretching. In effect, the sediments will be under- or over-sampled, while strati-

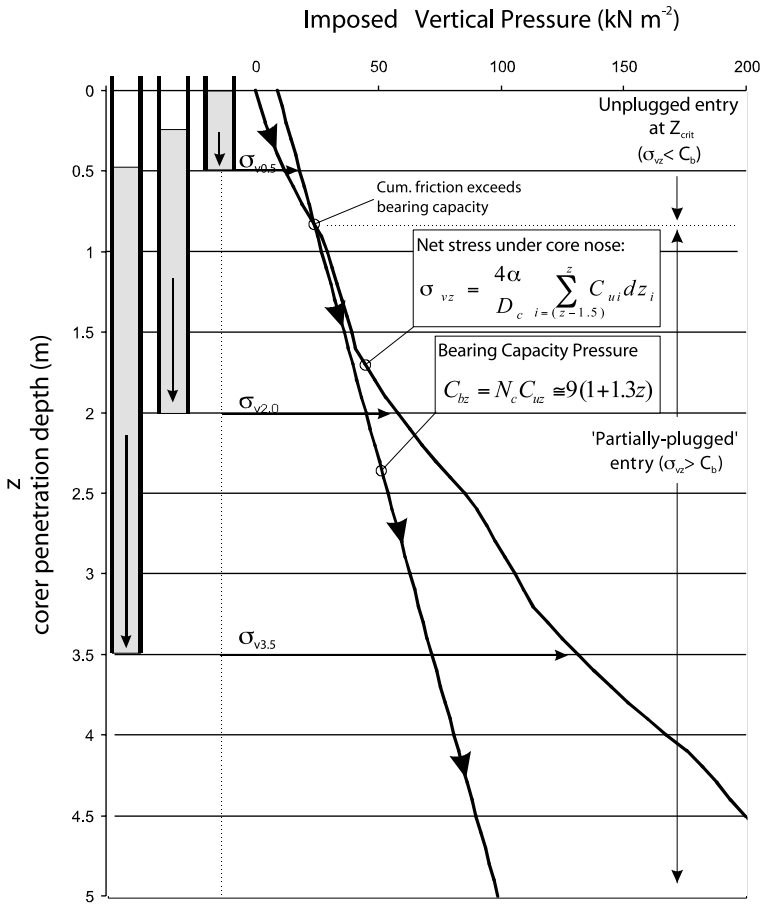

Fig. 2. The accumulation of sediment inside a descending core results in a vertical pressure beneath the corer. When this pressure eventually reaches equilibrium with in situ bearing capacity pressure (z_{crit}) it remains in equilibrium, with sediment entry continuing to the extent that this equilibrium is maintained. The pressure beneath the descending corer therefore follows the trajectory marked with arrows, above.

graphic integrity and wet-densities are preserved (Lebel et al., 1992; Emery and Dietz, 1941). Before cumulative friction comes to equal in situ bearing capacity pressure, this thinning is minor, and has been modelled here as an elastic response. After cumulative friction comes to equal in situ bearing capacity pressure, much greater sediment thinning ensues in order to maintain the balance of pressures, and is modelled here in terms of partially plugged tube sampling.

2.3. Piston cores: perfect and imperfect

Throughout this analysis of sediment–corer interactions, reference has been made solely to cylindrical and square gravity-type corers (i.e. simple open-ended tubes). Kullenberg-type piston corers, however, attempt to maintain a piston inside the core barrel at the level of the sediment–water interface so that the frictional drag between the barrel and the sediment core is counteracted by a low relative pressure maintained above the sediment column. A perfect piston corer, in contrast to a simple gravity corer, maintains lithostatic stress conditions at the core nose throughout the corer's penetration, leaving the sediments essentially undistorted (Fig. 3, I, II). Maintaining the piston immobile throughout the coring pro-

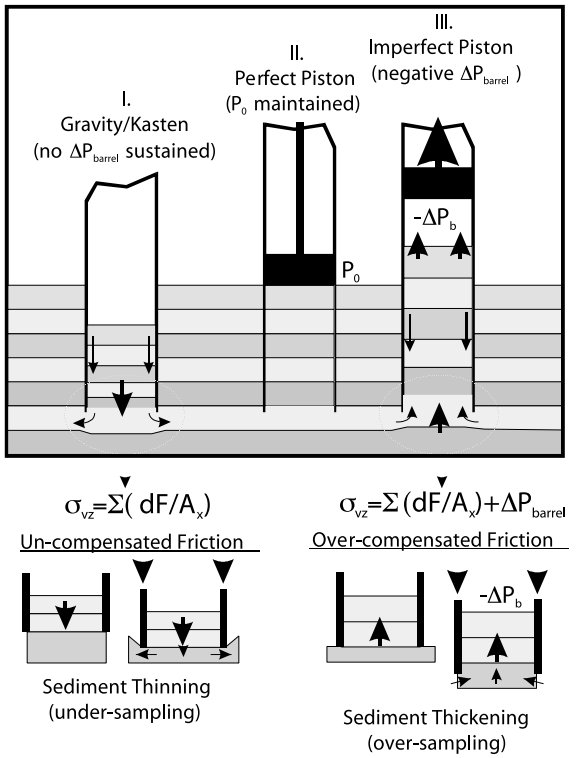

Fig. 3. Three possible coring scenarios: gravity-type, perfect piston (no piston acceleration), and imperfect piston (piston accelerates upward). Gravity-type coring may result in 'under-sampling', while imperfect piston coring may result in sediment 'over-sampling'.

cess, however, has proven very difficult to achieve in simple Kullenberg-type piston corers, with 'cable recoil' often cited as a likely culprit (McCoy, 1985; Buckley et al., 1994). Cable recoil describes a 'whiplash' effect in the coring cable, occurring when the cable is rapidly unloaded (figure 1 in McCoy, 1985). Thus the cable supporting the entire coring apparatus (weight, core head and barrel) is suddenly relieved of its load, either by triggering of the core-tripping mechanism or by impact of a gravity core with the seabed, and immediately retracts elastically if the core weight and cable length have been sufficient to produce a significant elastic extension. As the cable accelerates upwards it pulls the piston with it, creating a very low pressure inside the core barrel moving downwards through the sediment. Hence, the potential for cable recoil and upward piston movement during coring depends on the elastic extension of the coring cable caused by the weight of the entire coring apparatus. Currently, coring cables are commonly made of aramid fibres (a composite polymer similar to 'Kevlar'), which offer, among many advantages, very low elasticity (Young's modulus, $\lambda \sim 124$ GPa) and a density (~ 1450 kg m^{-3}) close to that of the sea-water in which they are immersed (Schilling et al., 1988). This renders them less prone to stretching than their steel precursors, and of low immersed weight when deployed at sea. The elastic extension of aramid cables depends on: the elastic modulus of the aramid fibres (λ); the length of cable deployed (l); and the total weight of the coring apparatus when immersed in sea-water. Simple dynamic analysis tells us that an elastic cable 'released' from its load at the time of triggering has an initial acceleration and maximum amplitude of oscillation given by:

$$a_i = -\left(\frac{g}{dl}\right) x_0 \text{ (acceleration)} \tag{11}$$

$$A_{max} = \frac{(M+m)gl_0}{\lambda} - dl \text{ (amplitude)} \tag{12}$$

where g is the acceleration due to gravity, λ is the elastic modulus of the cable, dl is the extension in the cable under its own immersed weight (m), l_0 is the original length of the cable ($\sim$coring water depth), and x_0 is the total extension of the cable under the added immersed weight of the coring apparatus (M). It is the acceleration and the amplitude of oscillation described above that determine the extent of piston recoil, and hence of negative pressure inside the core barrel. These equations show that although the near-weightlessness of an immersed aramid cable limits any 'standing extension' under its own weight, it also greatly enhances the cable's acceleration when the corer is released. This is particularly the case if, in contrast, the added weight of the coring apparatus does cause a large elastic extension in the cable. It is also apparent from the above analysis that the potential extent of cable/piston recoil is mainly determined by two important parameters: (i) the *water depth* at the coring location ($\sim l_0$);

and (ii) the *weight* of the coring apparatus (M). Hence, we expect cable recoil to be more problematic at deeper coring locations, and for heavier corers, whether of gravity or piston design. In the case of gravity corers, extreme cable recoil may result in the corer being pulled out of the sediments completely, causing double penetration (Weaver and Schultheiss, 1983; Shen et al., 2001). In piston corers it results in piston acceleration and imperfect piston coring (McCoy, 1985; Buckley et al., 1994). The above equations suggest that for coring operations at ~3000 m water depth, a typical maximum amplitude of recoil may be ~5–10 m if immersed resistance to cable recoil is ignored.

The effect of the piston moving upward with respect to the sediment top during the coring process would be to produce an excess negative pressure anomaly (with respect to sea-floor pressure) inside the core barrel above the sediment column entering the corer. The situation produces a syringe effect, and represents a drastic over-compensation for the downward frictional drag on the sediments. Such cable accelerations and pressure anomalies have indeed been observed (Buckley et al., 1994), and are often suggested by evidence such as core-liner collapse or mid-core flow-in.

The same set of stress–strain conditions already outlined for a simple gravity-type corer apply to any piston corer, though with a pressure function applied at the top of the soil column. In the case of a perfect piston corer, the evolving downward pressure anomaly above lithostatic stress ($\Delta\sigma_{vz}$, due to frictional drag) is compensated by an opposing barrel pressure anomaly with respect to sea-floor pressure (ΔP_b) provided by a fixed piston, so that ideally:

$$P_b(z) - P_d = \Delta P_b(z) = \Delta\sigma_{vz} \tag{13}$$

where $P_b(z)$ is the internal barrel pressure and P_d is the pressure at sea-floor depth. The barrel pressure evolves over time with corer penetration (z), matching the development of the downward pressure ($\Delta\sigma_{vz}$). In an imperfect piston, however, where the piston accelerates upward relative to the sea bed, a negative pressure anomaly develops above the soil column. The net downward stress (above in situ lithostatic pressure) imposed on in situ sediments below the base of the descending corer is given by:

$$\Delta\sigma_{vz} = \left(\frac{4\alpha}{D_c}\sum_{i=(z-1.5)}^{z} C_{ui}\mathrm{d}z_i\right) + \Delta P_b(t) \tag{14}$$

In this case, the barrel pressure drop ($\Delta P_b(t)$, negative with respect to $\Delta\sigma_{vz}$) evolves as a function of time, depending on the unique cable dynamics associated with cable recoil. It develops independently of the downward vertical stress due to friction ($\Delta\sigma_{vz}$), so that the sum of opposing pressures varies throughout penetration, producing different effects down-core. When the induced negative pressure is higher than the vertical frictional stress, a net upward (negative) pressure results beneath the descending corer, and hence exerts suction on the sediments being sampled. In response, the sediments will be 'over-sampled' (or 'thickened'). This effect may be as subtle as the sediment thinning described for gravity-type corers, or indeed may be so extreme as to produce mid-core flow-in, disrupting or even obliterating any primary sedimentary structures. Fig. 3 summarises the proposed effects of tube sampling for the three coring scenarios considered so far: gravity-type corers ('uncompensated' for friction), a perfect piston corer (compensated for friction), and an imperfect piston corer ('over-compensated' for friction). Identifying these effects in sediment cores is extremely difficult, particularly when they are too subtle to have destroyed the structural integrity of the core or the sediments are too homogeneous in appearance to betray any structural effects. Fig. 4 illustrates some more obvious or extreme examples of coring 'artefacts'. Lacking such clues, however, one is often at a loss in assessing the actual effects of the coring process on the dimensional and structural integrity of the resultant core, even though some deformation may be suspected. Magnetic fabric measurements often show deformation effects that are not visible macroscopically (Thouveny et al., 2000), though no calibration exists for an estimation of the amount of deformation. An assessment of the stratigraphic and dimensional integrity of a core requires some knowledge of the stratigraphic 'truth', which is generally inaccessible through standard sam-

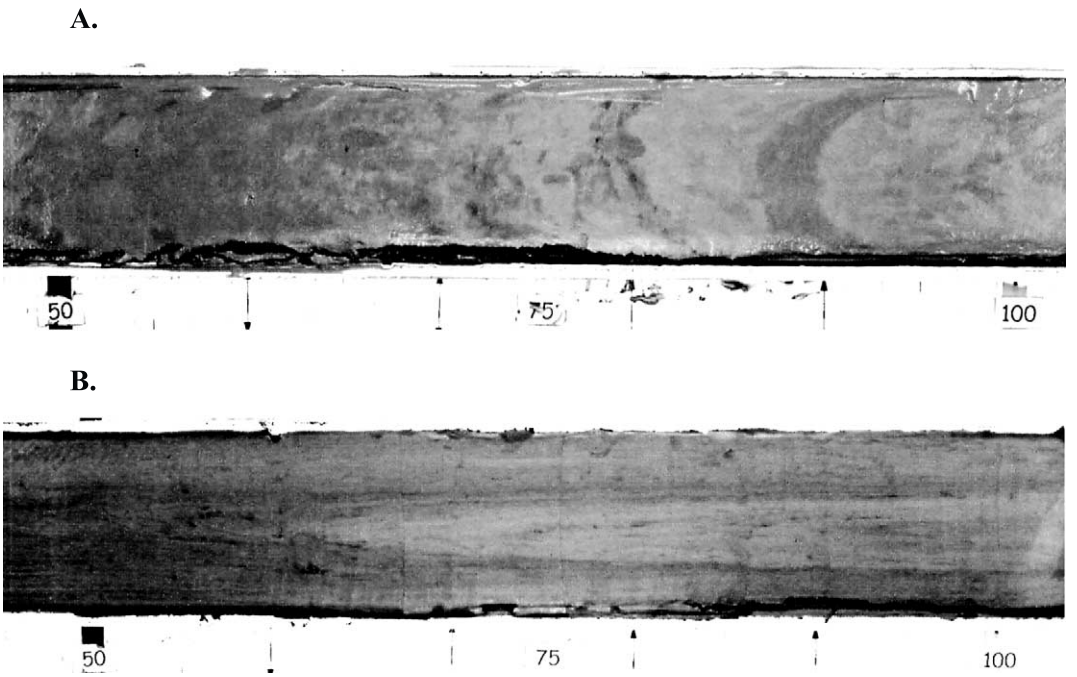

Fig. 4. (A) Bending of laminae in piston core (MD01-2446, section IIb). Apex of bent layer is thickened due to sediment flow (without pore-water flow). (B) Extreme suction in a piston core (MD01-2442, section XIXb), causing 'flow-in'. Complete vertical lineation or mottling (mixing) of sediments would ensue with greater suction.

pling techniques, given the ubiquity of sampling effects on in situ stratigraphy. A modelling approach based on soil mechanics is therefore proposed as a means to investigate the specific effects of various coring techniques on the dimensional integrity of the sediments they retrieve.

3. Applications

3.1. Materials and methods

Four cores retrieved by the N.O. *Marion Dufresne* from a single location (37°48′N, 10°10′W), at a water depth of 3146 m, will be used for comparison with modelled results for the coring process:

(i) the Cambridge *Kasten* core MD99-2334K (Kogler, 1963; Zangger and McCave, 1990; Labeyrie and Jansen, 1999), with a 7 m long square barrel of inner side length ('diameter') (D_i) 0.150 m and outer 'diameter' (D_o) 0.155 m, deployed with a 4 ton core-head weight ('Kasten');

(ii) the cylindrical gravity core MD01-2440, taken with a cylindrical pistonless Calypso corer ($D_i = 0.11$ m, $D_o = 0.20$ m) with a 2 ton weight (MD123 Geosciences Cruise, Leg 2, 2001) ('Gravity');

(iii) the cylindrical giant *Calypso* piston core MD95-2042 ($D_i = 0.11$ m, $D_o = 0.2$ m), taken with a 4 ton weight (Bassinot and Labeyrie, 1996) ('Heavy Calypso'); and

(iv) the giant Calypso piston core MD01-2441, taken with a 2 ton weight (Geosciences Cruise, Leg 2, 2001) ('Light Calypso').

All of these cores were deployed on aramid cables. For the Kasten core MD99-2334K, corer penetration was greater than the 7.00 m barrel of the corer (as indicated by mud having entered *into* the upper vents). However, only 5.50 m of sediment was recovered, with a 1.60 m void at the top of the upper section. In addition, a sharp horizon of oxidised sediments, similar to those at the core top, were identified at 1.07 m, suggesting double penetration (probably due to cable recoil) (Weaver and Schultheiss, 1983). The 20 m gravity corer

(MD01-2440) also recovered less than penetration, as indicated by a mud line at ~12 m on the outside of the corer compared to 6.97 m of sediment inside. In piston core MD95-2042 (which was bent during retrieval), of the total 39.56 m of sediment entry, only 32.5 m of sediment was recovered, with 7.06 m of sediment missing from the base of the core barrel and with the basal 2.5 m of the recovered sediment showing evidence of disturbance, most probably as a result of 'flow-in' (Cayre et al., 1999). Unfortunately, there is no information concerning the penetration of the 'light-weight' piston core MD01-2441, which recovered 14.15 m of sediment in a 20 m barrel.

Magnetic susceptibility and gamma-ray attenuation (wet-density) measurements were made on board the *Marion Dufresne* for both of the piston cores and the gravity core (Bassinot and Labeyrie, 1996; Labeyrie and Jansen, 1999). For the Kasten core MD99-2334K, magnetic susceptibility measurements were supplied by N. Thouveny (CEREGE, Aix en Provence, France), and water-content measurements were determined by weighing, desiccating and re-weighing 1 cm^3 bulk samples retrieved immediately after core retrieval. Organic and inorganic carbon content was also determined for the fine fraction (< 63 μm) of core MD99-2334K using a Carlo Erba EA 1106 elemental analyser. Precision for these analyses was better than 0.5%. The carbonate content of the samples was calculated by assuming that all inorganic carbon was in the form of $CaCO_3$.

The magnetic susceptibility records of these cores provide a sound basis for stratigraphic correlation, allowing the identification of key stratigraphic markers such as Heinrich events and glacial terminations (Thouveny et al., 2000). Based on such correlations, discrepancies in the stratigraphic dimensions in the cores indicate relative thickening or thinning of the in situ sediments due to the specific effects of each coring device. The four cores from the *Marion Dufresne* therefore provide the basis for a comparison with models of four coring scenarios:

(i) a square gravity corer (Kasten), $D_c = 0.15$ m;

(ii) a cylindrical gravity corer, $D_c = 0.10$ m;

(iii) a 'light and imperfect' cylindrical piston corer, $D_c = 0.1$ m, corer weight = W;

(iv) a 'heavy and imperfect' cylindrical piston corer, $D_c = 0.1$ m, corer weight = $2W$.

Eqs. 11 and 12 suggest that the cable accelera-

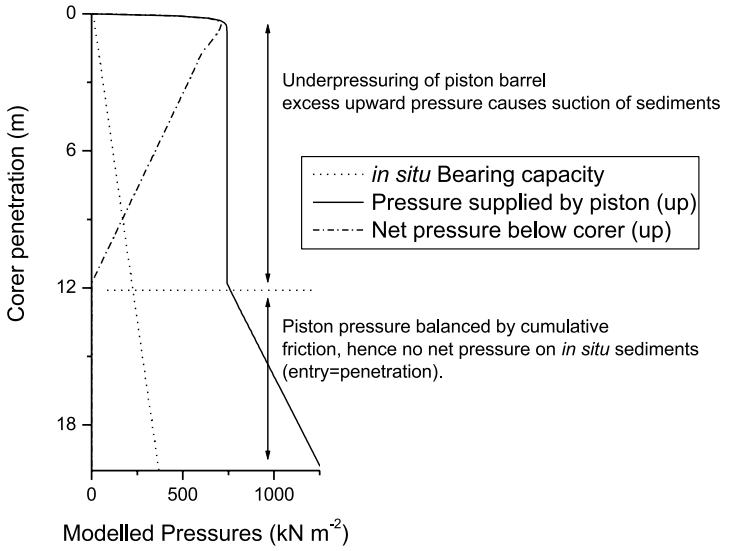

Fig. 5. Modelled pressures associated with imperfect piston coring (shown here for the 'light piston core'). Barrel pressure drops rapidly (shown here as a positive *upward* pressure deviation) in response to upward piston acceleration. This results in suction at core base, until cumulative friction inside the corer balances the friction and equilibrium is then maintained, allowing 'perfect' piston sampling below the equilibrium depth.

tion in the two piston cores scales as the ratio of the core weights and lengths. The above coring scenarios have been modelled for a single coring depth, or cable length. Hence, the heavy piston core will be modelled as having double the cable acceleration, and hence double the pressure anomaly, of the lighter piston core. Defining the pressure function that would apply to the top of the piston core is particularly problematic. Measurements of barrel pressures during the retrieval of relatively shallow cores (Buckley et al., 1994) have indicated drops in pressure of up to ~750 kPa. These developed rapidly in response to piston/cable accelerations, and tended to accumulate throughout penetration as they were only partially attenuated by sediment over-sampling. Indeed, measurable negative pressure anomalies only develop inside the corer when the piston accelerates upward and sediment does *not* 'flow in' to satisfy the pressure imbalance. Hence, efficient over-sampling of sediments (sediment thickening or even flow-in) need not actually be associated with large pressure anomalies, and may only reliably be identified by entry–penetration comparisons. In modelling the barrel pressure for an imperfect piston corer, a maximum pressure anomaly of −750 kPa has been applied to the light piston core with a 2 ton weight, with pressure increasing rapidly from zero until it is balanced by the increasing frictional drag. The piston pressure then tracks the frictional drag (as in a perfect piston corer), as the piston ceases to accelerate with respect to the top of the sediments (Fig. 5). For simplicity, the attenuation of pressure by entry of extra sediment into the core barrel has been ignored. For the heavy piston corer, twice the pressure deficit of the light piston corer is assumed based on an expected two-fold factor of cable recoil (see above).

3.2. Stratigraphic results

A close analysis of X-radiograph and total fine $CaCO_3$% (TFC%) records confirms the suspected double-sampling of the upper 107 cm in the Kasten core MD99-2334K (Fig. 6). The repeated stratigraphy is immediately obvious and likely represents the effect of cable recoil. An X-radiograph

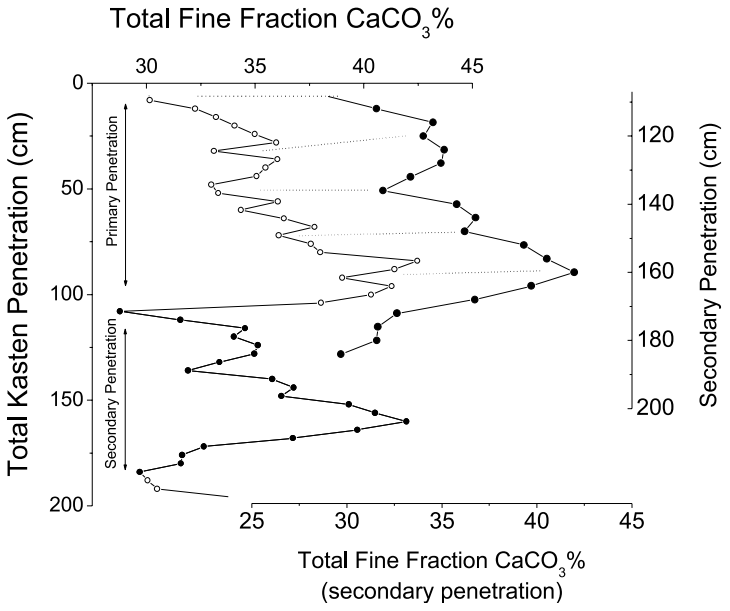

Fig. 6. Double recovery of stratigraphy in Kasten core MD99-2334K, expressed in the TFC% record. Secondary penetration (the repeated interval) is re-plotted beside the primary penetration showing correlation points used to determine the shortening ratio for secondary recovery relative to primary recovery. This provides an upper limit on the shortening ratio of primary recovery relative to in situ stratigraphy.

of the re-penetration horizon is shown in Fig. 7, in which the density increase across the horizon can also be seen as well as a slip plane indicating structural damage. Re-penetration artefacts such as this indicate the powerful upward acceleration that may be generated as a result of cable recoil, providing enough force to halt the corer's descent and pull it (and its 4 ton weight) completely out of the sea floor. Fine-scale features of the TFC% record allow comparison of the dimensions of the primary and secondary recovery of the repeated section (Fig. 8). This shows that the uppermost 8 cm of sediment has been skipped during secondary recovery and that the repeated interval has been shortened by ~20% on average (average filling factor (AFR) ~0.8). IFRs, however, indicate that all of this relative shortening has been concentrated in three intervals of 40–60% recovery, with the majority of secondary recovery being unshortened. The under-sampling of the repeated stratigraphy in MD99-2334K provides us with a maximum estimate of the actual core-average thinning associated with Kasten tube sampling, equal to ~20% (similar to Parker and Sills (1990)). Observations of cylindrical gravity core re-penetration (Shen et al., 2001) may provide a similar upper estimate for under-sampling in such corers, equal to ~53%. These estimates are much higher than for normal uninterrupted penetration due to: (i) the need to overcome a *static* (hence greater) friction between the upper soil section and the corer; and (ii) generally greater friction between soil and corer resulting from a higher (uncontrolled free-fall) entry velocity during re-penetration. The 'undulatory' character of the relative thinning relationship is notable, and results

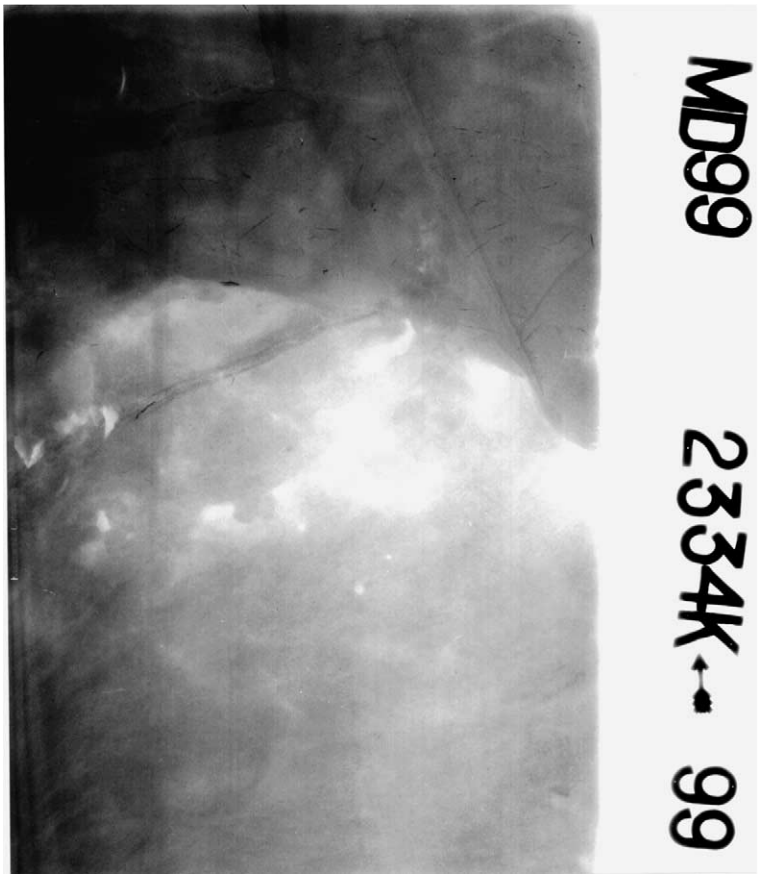

Fig. 7. X-radiograph of re-penetration horizon in Kasten core MD99-2334K. Darker colours represent denser sediment.

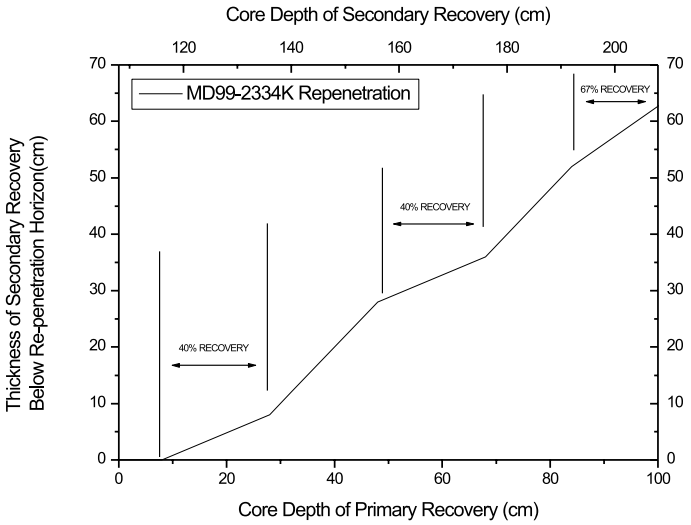

Fig. 8. Shortening of secondary penetration in the Kasten core MD99-2334K relative to primary penetration. An average shortening (1−AFR) of ∼20% has resulted from alternating intervals of 100% and 40–60% recovery. The 20% shortening provides an upper limit on the shortening experienced by an uninterrupted Kasten core, and allows the repenetrated core to be modelled.

from the changing balance between in situ bearing capacity and cumulative friction. In correcting for the re-penetration in MD99-2334K, tie points have been chosen to exclude the repeated and disrupted sediments between 78 and 154 cm (see Fig. 6). Henceforth all depths for core MD99-2334K will refer to 'corrected' apparent stratigraphic depths in the spliced core.

Stratigraphic correlation, based on magnetic susceptibility, of the four cores retrieved by the *Marion Dufresne* is illustrated in Fig. 9. This shows that the recovered length of the same stratigraphic record, deposited at a single location, may vary by a factor of up to 2.7. This is due solely to the various distortional effects of each coring method.

3.3. Modelling results and discussion

In Fig. 10A, the depths of the cores are plotted against that of the longest core, MD95-2042, along with the modelled results for the four coring scenarios. Fig. 10B compares the core length–penetration relationships for the four cases, illustrating their deviation from 1:1, or ideal frictionless coring. Of course, for the real examples, no measure of the actual relationships between each core's dimensions and the 'true' dimensions of the stratigraphy is available (as is shown in Fig. 10B for the modelled responses). This provides the very incentive for adopting a modelling approach, where the reconstruction of the dimensional relationships between the various core types may tell us something about the dimensional relationships between each core type and the in situ stratigraphy. Indeed, in modelling the coring process, the primary motivation is less to accurately reconstruct a complex reality than to identify only the most salient aspects of that reality. Here, the main objective is to test the assumptions that underpin our conceptual understanding of tube sampling and to investigate important parameters that may previously have been underestimated or overlooked.

As one might expect, the gravity-type corers contain shorter stratigraphies than do the piston cores, with the cylindrical gravity corer exhibiting the greatest amount of relative shortening and the heavy piston corer the greatest relative extension. The modelled responses, insofar as they reproduce the correct type of depth–depth relationships *between each core type*, compare very well with the real records. However, of the coring scenarios, the relationships between the two piston cores, and

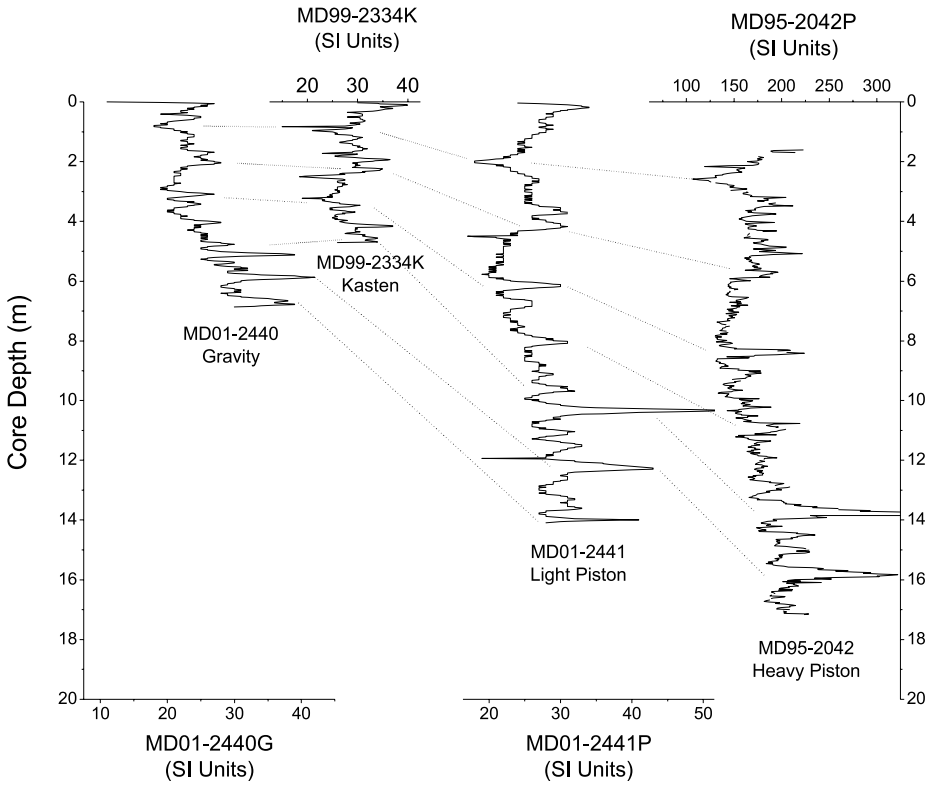

Fig. 9. Correlation of four cores from the Iberian Margin based on magnetic susceptibility records. From left to right: MD01-2441 gravity, MD99-2334K Kasten, MD01-2440 light piston, MD95-2042 heavy piston. Note anomalous calibration of MD95-2042 magnetic susceptibility possibly due to problems with shipboard density determination (Bassinot and Labeyrie, 1996).

between the re-penetrating Kasten core and the heavy piston core, have proven most difficult to reproduce. In the case of the piston cores, the reason for this is the uncertainty involved in accurately reconstructing the cable–piston dynamics during the coring procedure. These factors control the pressure function that is applied to the core top during penetration, a parameter to which the model is very sensitive, particularly for very large pressure drops. Hence, it is clear that the response of sediments to imperfect piston sampling is highly dependent on the specific, perhaps highly unpredictable, piston–cable dynamics on any given coring operation. Nevertheless, it appears that the general controls on cable recoil, and hence the potential for piston acceleration resulting in over-sampling, have been adequately represented. Longer, lighter, more elastic cables carrying heavier core assemblies tend to result in greater cable accelerations upon triggering, offering the potential for proportionately more over-sampling due to under-pressuring and piston suction during core retrieval.

The same cable recoil also increases the likelihood of Kasten/gravity core double penetration, which is what has complicated the modelling of the Kasten core recovery. In this case, the double penetration of the Kasten corer is associated with lower recovery ratios than modelled for normal penetration. The comparison of the primary and secondary recovery lengths made above, backed up by similar observations made by Weaver and Schultheiss (1983), leads us to suggest that the reasons for poor secondary recovery are two-fold. Firstly, it is more difficult to re-initiate soil entry, as a static wall friction between the initial soil plug and the core walls must be overcome before secondary recovery ensues (e.g. Paik and

Lee, 1993). Secondly, an increased (uncontrolled) speed of entry, following cable recoil, may result in a higher effective friction factor between the sediments and the core barrel. Reduced entry ratios (i.e. effectively higher skin friction factors) have indeed been observed for more rapid penetration velocities of Kasten corers (Parker and Sills, 1990). This may represent the result of higher strain rates resulting in higher resistance to shear and perhaps less effective mud-slick development. If we apply the 80% recovery factor determined for the repeated interval of the Kasten MD99-2334K to the modelled recovery for uninterrupted Kasten penetration, a very good fit is obtained between model and observations (except for the basal 1 m of recovery, which appears to have been affected by severe plugging). The double penetration of the 4-ton Kasten core illustrates two points: the immense forces associated with cable rebound; and the acute sensitivity of soil recovery to changes in the effective friction factor between soil and corer (particularly in pistonless gravity-type corers).

Modelled incremental- and cumulative average filling ratios (IFRs and AFRs) for the gravity-type cores (shown in Fig. 10C) compare well with values measured in real coring scenarios. Parker and Sills (1990) report AFRs of ~0.5–0.80 for gravity- and Kasten-type cores. Their results indicate that Kasten corers tend to produce AFRs closer to ~0.75 for ~2.4 m penetration, and cylindrical gravity corers tend to produce AFRs closer to ~0.60 for ~3.0 m penetration. The modelled Kasten corer (uninterrupted penetration) produces an AFR of ~0.9 for 2.4 m penetration, while the modelled cylindrical gravity corer produces an AFR of ~0.6 for 3.0 m penetration. Modelled results suggest ultimate AFRs tending towards ~0.5 for the cylindrical gravity corer and ~0.7 for the Kasten corer (without double penetration). This agrees with observation of mud-lines on long gravity corers and uninterrupted Kasten corers (Emery and Dietz, 1941). As pointed out by Parker and Sills (1990), the use of *average* filling ratios (AFRs) masks the variability of instantaneous sediment entry, which is faithfully recorded by *incremental* filling ratios (IFRs). The modelled response of the sediments suggests that the variability of IFRs represents the semi-plugged entry of soil into the descending corer, maintaining the balance between in situ bearing capacity and cumulative sediment–barrel friction. If the model is applied to a larger-diameter square barrel corer ($D_c > 20$ cm), the recovery ratios are greatly enhanced, with an ultimate AFR > 0.9, rather than ~0.7 for $D_c = 15$ cm. Increasing the diameter of the cylindrical gravity corer from 10 to 15 cm produces an ultimate AFR of ~0.7, a recovery as high as the present Kasten design. Hence corer diameter plays an important role in increasing the sediment recovery/penetration ratio.

Unfortunately, we know of no published IFR or AFR data for piston cores, precluding a comparison of modelled and measured filling ratios. However, modelled results suggest that, depending on the magnitude of the pressure drop inside the core barrel, IFRs may be as high as ~1.90–2.75 near the top of the core, and that AFRs tend gradually towards ~1.0 with increasing penetration (Fig. 10C). Whether or not 'ideal' behaviour (incremental sediment entry equals incremental penetration, slope = 1 in Fig. 10B) actually ensues, depends on the specific pressure history of the coring operation. However, the progression towards a 1:1 length relationship between the two real piston cores (MD95-2042 and MD01-2441) supports the suggestion that piston cores do indeed trend towards 'ideal' behaviour. The point at which this occurs represents a balance between the cumulative friction inside the corer and the reduced barrel pressure above the sediments, causing the piston to cease moving with respect to the sediments. This transition point, from net 'suction' to balanced vertical pressures, defines a depth below which the stratigraphy is essentially intact, having suffered no over-sampling through sediment 'flow'.

Modelled responses for the light and heavy piston cores suggest balance depths of ~8 and ~10 m, respectively. This is consistent with magnetic anisotropy measurements made on piston core MD95-2042 by Thouveny et al. (2000), which show a transition from a dominantly horizontal magnetic fabric deeper than ~10–15 m to a dominantly vertical fabric shallower than ~10–15 m.

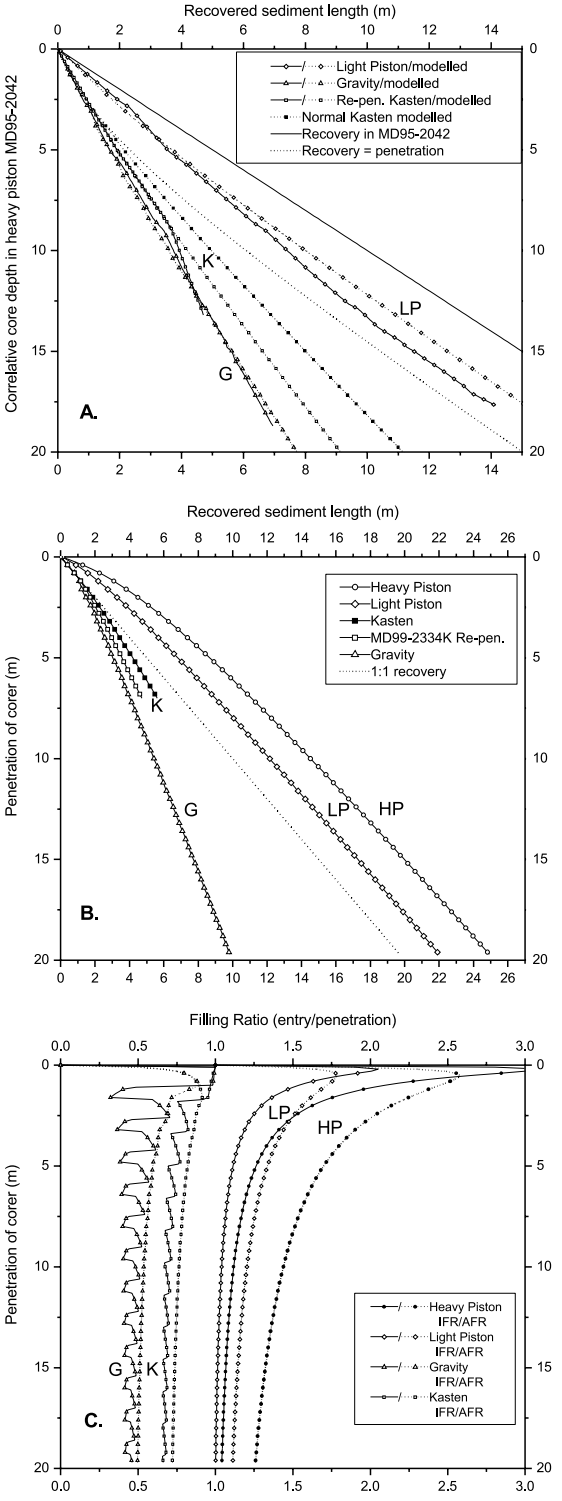

This transition has been interpreted as a change from normally consolidated sediments lower down in the core, to extensionally (vertically) strained sediments in the upper ~10 m of the core. The same transition point is reflected here in terms of a balance between piston pressure and cumulative soil–corer friction, producing an attenuation of sediment over-sampling. A similar effect has been observed in piston cores MD95-2039 and MD95-2040 (Thouveny et al., 2000) and is related to discrepancies between sedimentation rate estimates based on stratigraphic thickness and on $^{230}Th_{xs}$ profiles (Thomson et al., 1999; Hall and McCave, 2000). It is noteworthy that the magnetic fabric transition depth is shortest in the shallowest of the cores (~8 m in MD95-2040; 2465 m water depth) and longest in the deepest of the cores (~14 m in MD95-2039; 3381 m water depth) (Moreno et al., 2002), supporting the suggested link between longer coring

Fig. 10. (A) Comparison of modelled and real length relationships between the four core types, shown on the depth scale of the heavy piston core (real equivalent is MD95-2042). This emulates the perspective one actually has when comparing the stratigraphic lengths of various cores from a single location (continuous penetration measurements unavailable). The model successfully reproduces the observed inter-core relationships (particularly for the gravity core and the re-penetrating Kasten core modelled using the 80% recovery inferred from repenetration recovery ratios). Accurately defining the evolution and magnitude of the piston barrel pressure is problematic. The light piston core MD01-2441P trends toward entry ratios equal to those in the heavy piston core MD95-2042, possibly indicating 'perfect' sampling at the bases of these cores. (B) Modelled sediment penetration versus sediment recovery for gravity-, Kasten, light piston and heavy piston coring scenarios. Gravity-type corers sample perfectly at first and trend towards ~0.5 entry ratios. Kasten corers do not exceed 7 m length. Piston cores that over-sample in their upper sections (in response to under-pressuring) tend towards complete recovery (i.e. entry = recovery) in their lower sections. (C) Modelled IFRs and AFRs for the four coring scenarios. Gravity-type corers tend towards filling ratios of ~0.5, while piston corers trend towards filling ratios of ~1.0. The oscillation of IFRs in the Kasten and gravity cores is notable, representing 'semi-plugged' sampling (see text). The over-sampling of piston corers drops off rapidly with sediment recovery due to cumulative sediment–corer friction, resulting in an effective transition to undisturbed sampling below ~10–15 m, depending on magnitude of barrel pressure drop.

cables and greater piston acceleration. In gravity cores, the compressive equivalent of the piston transition depth is the point at which the cumulative friction inside the barrel equals the bearing capacity of the in situ sediments, and 'partial plugging' ensues. This occurs relatively shallow in gravity-type cores and depends primarily on the skin friction factor between the corer and the sediments, which in turn is related to sediment water content and lithology (clay vs. carbonate) which are the main controls on sediment shear strength.

The linearity of all of the depth–depth relationships is notable. This important characteristic of the depth–depth relationships is reproduced in the soil response models through the limited frictional contribution of the upper portion of the sediment column in the corer. Hence, it appears that some attenuation of the cumulative sediment-tube friction is an important feature of the model. As suggested above, this could be attributed to the smearing of marginal sediments up-core, causing less than the total side-wall friction to contribute to the pressure at the core base. This also causes less friction to be *generated* between the core barrel and the mobilised marginal sediments, which have lower 'ultimate/mobilised' shear strengths and may even be reduced to a liquid slurry. Alternatively, or additionally, an increase in the lateral pressure towards the base of the core may be generated as a result of imposed vertical compression. This may help to maintain greater friction at the base of the core by imposing a greater normal force against the corer walls. Without an attenuation of friction up-corer, stress–strain relationships predict that the gravity-type corers would 'plug' completely ($\sim$zero entry) after only $\sim$1–2 m penetration (for $\alpha \sim 0.35$), which is generally not observed.

3.4. Implications for palaeoceanographic studies

The extent and character of dimensional distortion during coring bears directly on sampling limits, sediment–core fabric, and depth–age relationships. As demonstrated by Thouveny et al. (2000), over-sampling in piston cores seriously affects magnetic fabric measurements, particularly in the upper portions of piston cores. The vertical re-alignment of magnetic particles is achieved as sediment flows inward at the core tip (note that this plastic flow of sediment has been approximated by an elastic response in the soil deformation model above). Significant vertical strains and sediment inflow may be obtained in piston cores (such as MD95-2042 or MD01-2041) without destroying the stratigraphic integrity of the sediments. In such cases, the sediment may be 'over-sampled' in a quasi-continuous manner over scales of decimetres to metres, depending on local variations in lithology. Perhaps more subversive is the likelihood that softer (higher water content) layers would be more over-sampled than harder ones, with the opposite effect occurring in gravity cores, as suggested by the variable IFRs in MD99-2334K (Fig. 8). This mode of deformation is most likely to be missed for a lack of visibly deformed laminae. Indeed, in sediments less prone to lateral flow, such sediment 'thickening' may be replaced by a non-conservative bending of laminae (i.e. sediment flows toward the apex of the anticline from its limbs, or is drawn out from the limbs by 'smearing'). This mode of sediment response is more often noted, for it results in observable secondary structures (Fig. 4A). In the case of extreme sediment deformation, the primary sedimentary fabric is completely obliterated, producing the vertically lineated sediment typical of classic 'flow-in' (Fig. 4B). Records of physical properties, such as bulk magnetic susceptibility or shear strength, exhibiting a sudden drop to flat 'average' values (or lower 'ultimate' shear strengths) may also indicate piston core flow-in.

The potential by-passing of the uppermost loosely consolidated sediments has long been documented in many piston cores, particularly by comparison with pilot gravity cores (e.g. Ross and Riedel, 1967). This mode of sediment skipping depends primarily on the area ratio of the core cutter and its role in focussing the weight of the corer. However, in imperfect piston corers, where the piston accelerates upwards, this effect is likely to be avoided. Furthermore, with increasing penetration, piston corers are not generally expected to suffer sediment by-passing unless the piston is able to move downward with the sedi-

ment. In contrast, cylindrical gravity-type corers (as modelled above) appear inevitably to tend towards an ultimate IFR of ~0.5. This is the compressive counterpart of 'thickening' in piston cores, resulting in a condensed yet still continuous stratigraphy. This does not appear to have any effect on magnetic anisotropy measurements (Thouveny, personal communication, 2001).

Dimensional distortion skews our estimates of age–depth relationships, and hence sedimentation rates and mass fluxes, bearing on our interpretations of sedimentary processes. The rapidity of the sampling process and the low permeability of fine-grained marine sediments ensure that undrained conditions are maintained, and that sediment densities are not affected during sampling. Absolute wet-density profiles for the four Iberian cores are not strictly comparable due to the different methods and/or calibrations used to determine them. However, a comparison of down-core wet-density trends expressed in standard deviation units (Fig. 11) suggests that none of the four cores exhibits drastically different profiles, although some noticeable differences are apparent. Thus the gravity-type cores exhibit rather similar profiles, and often exhibit opposite apparent density deviations to the piston cores (apparent density deviations exhibited in the gravity-type cores are either not exhibited or opposed in the piston cores). These wet-density discrepancies (taken at face value) do not appear to be consistently associated with any changes in the depth relationships of the cores, and are not likely to represent actual compression/dilation of the sediments during retrieval. Rather, they may represent late-stage (post-retrieval) re-equilibration of pore-pressure anomalies that have been maintained as a result of over- or under-pressuring during the sampling process. Under-sampling increases the pore pressures of sediments, while under-pressuring reduces them, and these pressure anomalies may eventually be relaxed by pore-fluid flow in the hours between core retrieval and shipboard density analyses.

Given that porosity must be maintained during coring (if not necessarily after core retrieval), sediment thinning and thickening will be associated with lower and higher apparent sedimentation rates, respectively. A comparison of the sedimentation rates exhibited by each of the four Iberian Margin cores described has been made by placing them all on the timescale of MD95-2042 (Shackle-

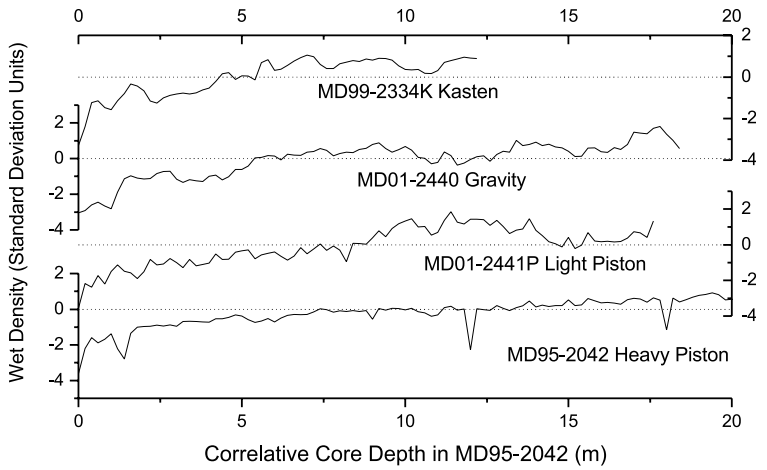

Fig. 11. Wet-density profiles for the four Iberian Margin cores. Standard deviation units (with respect to each core's average wet density) are used because of the incompatibility of the density methods/calibrations used for each core. Densities for the piston and cylindrical gravity cores are based on gamma-ray attenuation measurements (obtained on different cruises), while densities for the Kasten core are based on gravimetry. The rapidity of the sampling process and impermeability of the fine sediments precludes pore-water flow (density change) during sampling. Hence differences between the density profiles may have resulted from late-stage (post-recovery) equilibration with over-/under-pressuring incurred during sampling. These density differences give cause for concern in inference of mass flux in different cores.

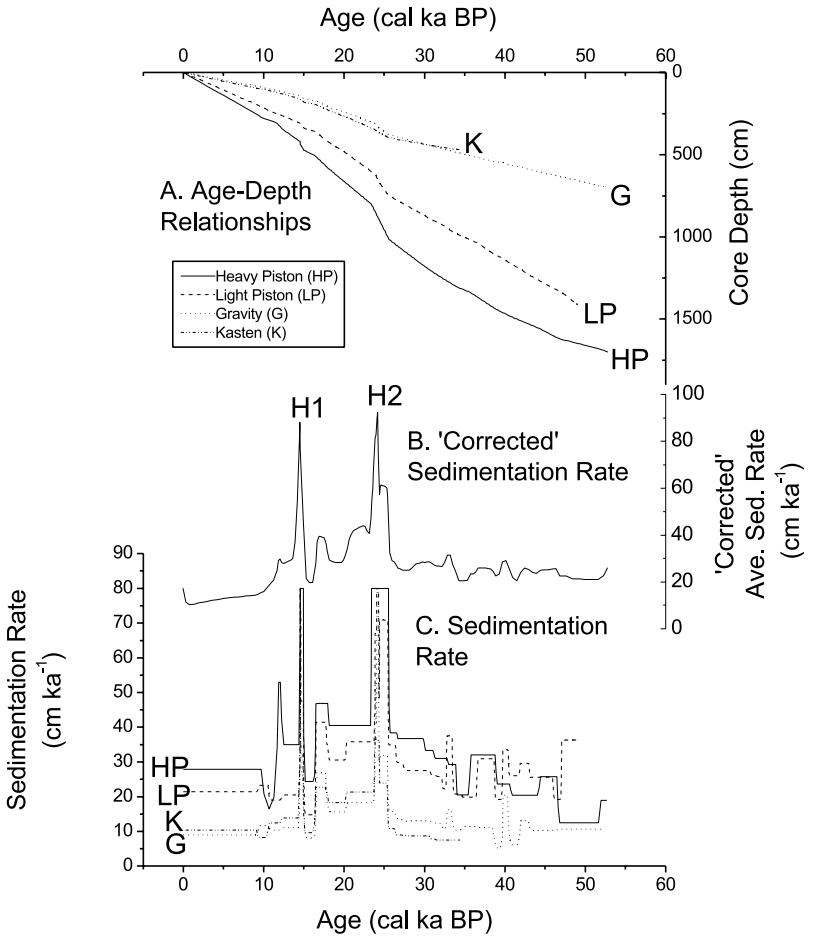

Fig. 12. Age–depth relationships and apparent sedimentation rates (A,C) for the four Iberian Margin cores (age scale based on correlation with SU81-18 and GRIP $\delta^{18}O_{ice}$, following Shackleton et al. (2000)). Over-sampling and under-sampling have produced discrepancies between the cores' depth–age relationships. True sedimentation rates may be best approximated by splicing the most 'intact' intervals of each core type. A 'corrected' sedimentation rate record may also be derived by applying the iterative soil response model, as shown in plot B. This suggests average sedimentation rates $\sim$32.0 cm ka^{-1} (24.8 cm ka^{-1}, excluding Heinrich events 1 and 2, which may be identified using magnetic susceptibility records (Thouveny et al., 2000)), and hence average fluxes of $\sim$22.8–29.4 g cm^{-2} ka^{-1} for an average dry bulk density $\sim$0.92 g cm^{-3}.

ton et al., 2000) (Fig. 12). In situ stratigraphic dimensions are most faithfully represented in the upper portions of gravity-type corers and in the lower portions of (imperfect) piston cores. Of course, piston cores that function perfectly contain the best representation of the stratigraphy all the way down-core, with the exception of the uppermost sediments, which may be by-passed. For the set of cores in Fig. 12, a spliced record of sedimentation rates may be most historically representative. However, there still remains a poorly sampled interval due to significant under-sampling deeper than $\sim$4 m in gravity cores and significant over-sampling shallower than $\sim$10 m in piston cores, or between $\sim$25 and 35 ka in this case. Nevertheless, Fig. 12B illustrates an average 'corrected' sedimentation rate record obtained by removing the sampling artefacts modelled for each coring scenario. A generalised quantitative expression for the 'correction' of extensional arte-

facts in all Kullenberg-type piston cores (such as Calypso cores) has not been attempted here, in part because the iterative character of the soil response model is not easily amenable to a precise solution. Nevertheless, the model described here is simple enough to be applied to any particular scenario, to which it may provide a consistent solution (as it has here) or by which it may be refuted. Indeed the identification of a single instance where cable rebound and extensional deformation has not occurred (using other core comparisons or magnetic susceptibility anisotropy measurements) would rule out the general applicability of this model, though it would not necessarily rule out its specific applicability in this or other cases.

It is worth noting that in many studies dimensional integrity can be less important than stratigraphic integrity, in which case sediment thickening may in fact represent an advantage. Thus, it may be extremely useful for the purposes of reconstructing high-resolution multi-proxy palaeoceanographic records to have a thickened (though stratigraphically intact) sedimentary record. However, such a record would tend to overrepresent (in thickness) the more rapidly deposited (more water-saturated and hence weaker) soil horizons, exaggerating down-core differences in sedimentation rate and creating only a discontinuous increase in resolution, for which cyclic phenomena would be misrepresented on linear age models with few age constraints.

The discrepancy between mass fluxes calculated from length–time relationships and from $^{230}Th_{xs}$ in cores MD95-2039 and MD95-2040 (Thomson et al., 1999) is a case in point where piston oversampling has contributed to stratigraphic artefacts. While dimensionally derived sedimentation rates are directly dependent on changes in the length of the stratigraphic record, Th_{xs} measurements are not, being controlled by actual ^{230}Th fluxes and fixed activity constants (Bacon, 1984). Modelling results here suggest that of the ~eightfold discrepancy between these sedimentation rate proxies in cores MD95-2039 and MD95-2040, ~25–30% can be explained by piston over-sampling, leaving ~75% of the discrepancy attributable to additional sediment supply, most likely from down-slope transport.

4. Summary and conclusions

In this paper we have analysed the effects of gravity- and piston coring techniques on soft sediment cores. Given that in situ stratigraphic dimensions are generally unavailable for comparison with recovered cores (lacking down-hole logs), a soil-response model has been constructed based on soil-mechanics principles. Using this model to reconstruct the expected depth relationships between Kasten-, cylindrical gravity-, and piston cores, and comparing them to real instances, it has been possible to test our assumptions of sediment response to tube sampling. These comparisons suggest that cable recoil is most likely responsible for piston acceleration resulting in suction, as proposed by Buckley et al. (1994). It appears that the extent of piston over-sampling, and the interval of sediment affected, are directly related to the weight of the coring apparatus and the length and elasticity of the coring cable. Heavier corers on lighter, longer, more elastic cables are predicted to suffer more over-sampling over a greater interval of stratigraphy. The actual interval of sediments affected by piston over-sampling is controlled by the extent of under-pressuring in the core barrel balanced against the cumulative friction between corer and sediments. A transition in the dominant magnetic fabric of the sediments may be used to identify the interval of over-sampled sediments (Thouveny et al., 2000), below which piston cores are likely to provide essentially intact samples of the in situ stratigraphy. The depth of the transition interval extends between ~5 and 15 m (depending on cable length) for the Calypso corer on a Kevlar cable. The same cable recoil that produces piston oversampling may also be responsible for the 'pull-out' and double penetration of gravity-type cores, as illustrated by the Kasten core MD99-2334K. Secondary recovery during re-penetration enhances the stratigraphic 'thinning' generally exhibited by gravity-type corers, providing an extreme upper limit on the average shortening associated with uninterrupted penetration (~20%). Stratigraphic thinning increases with deeper penetration, with essentially intact sediments being recovered down to ~3 m penetration. Typical design

parameters suggest that ultimate core average and IFRs in cylindrical gravity- and Kasten corers tend towards ~0.5 and 0.7, respectively, consistent with field observations (Parker and Sills, 1990). Until a truly practical design of recoilless piston core is successfully developed and promoted, the combination of different core types taken in parallel appears to be the most representative method of marine sediment sampling. Given the individual effects of the different coring apparatus analysed here, and their variability down-core, we suggest that a combination of a large-diameter (20–30 cm) square-barrel gravity corer for the upper 10–12 m of penetration, combined with a cylindrical piston corer for deeper penetration may provide the least deformed sample of in situ stratigraphy.

Acknowledgements

We are grateful to Dr David White of the Engineering Department for advice on pile-driving and model formulation, and to all those responsible for measuring and calibrating the shipboard magnetic susceptibility and water-content data, especially Drs N. Thouveny and I.R. Hall. We also record our thanks for the indispensable expert collaboration of Yvon Balut and his coring team on board *Marion Dufresne*.

References

Bacon, M.P., 1984. Glacial to interglacial changes in carbonate and clay sedimentation in the Atlantic Ocean estimated from ^{230}Th measurements. Isot. Geosci. 2, 97–111.

Bassinot, F., Labeyrie, L., 1996. IMAGES MD 101 a bord du Marion Dufresne du 29 mai au 11 julliet 1995. Inst. Français pour la Recherche et la Technologie, 96-1.

Blomquist, S., 1985. Core sampling of soft bottom sediment - an in situ study. Sedimentology 32, 605–612.

Bouma, A.H., Boerma, J.A.K., 1968. Vertical disturbances in piston cores. Mar. Geol. 6, 231–241.

Buckley, D.E., MacKinnon, W.G., Cranston, R.E., Christian, H.A., 1994. Problems with piston core sampling: Mechanical and geochemical diagnosis. Mar. Geol. 117, 95–106.

Cayre, O., Lancelot, Y., Vincent, E., Hall, M., 1999. Paleocean reconstructions from planktonic foraminifera off the Iberian Margin: temperature, salinity and Heinrich events. Paleoceanography 14, 384–396.

de Nicola, A., Randolph, M.F., 1997. The plugging behaviour of driven and jacked piles in sand. Geotechnique 47, 841–856.

Driscoll, A.H., Hollister, C.D., 1974. The W.H.O.I. giant piston core; state of the art. In: National Needs and Ocean Solutions; Oceanographic Instrumentation Techniques. Mar. Tech. Soc., Washington, DC, pp. 663–676.

Emery, K.O., Dietz, R.S., 1941. Gravity coring instrument and mechanics of sediment coring. Bull. Geol. Soc. Am. 52, 1685–1714.

Emery, K.O., Hulsemann, J., 1964. Shortening of sediment cores collected in open-barrel gravity corers. Sedimentology 3, 144–154.

Ericson, D.B., Wollin, G., 1956. Correlation of six cores from the equatorial Atlantic and the Caribbean. Deep-Sea Res. 3, 104–125.

Hall, I.R., McCave, I.N., 2000. Palaeocurrent reconstruction, sediment focussing on the Iberian margin over the last 140 ka. Earth Planet. Sci. Lett. 178, 152–164.

Hollister, C.D., Silva, A.J., Driscoll, A.H., 1973. A giant piston corer. Ocean Eng. 2, 159–168.

Kogler, F.C., 1963. Das Kastenlot. Meyniana 13, 1–7.

Kullenberg, B., 1947. The piston core sampler. Sven. Hydrogr. Biol. Komm. Skr. Ny Ser. Hydrogr. 3, 1–46.

Kullenberg, B., 1955. Deep-sea coring. Rep. Swed. Deep-Sea Exped. 4, 35–96.

Labeyrie, L., Jansen, E., 1999. Campagne INTERPOLE MD 114/IMAGES V a bord du Marion-Dufresne tome 3: Leg 5. l'Institut Francais pour la Recherche et la Technologie Polaires.

Lebel, J., Silverberg, N., Sundby, B., 1982. Gravity core shortening and pore water chemical gradients. Deep-Sea Res. 29, 1365–1372.

McCoy, F.W., 1985. Mid-core flow-in: implications for stretched stratigraphic sections in piston cores. J. Sediment. Petrol. 55, 608–610.

McCoy, F.W., 1980. Photographic analysis of coring. Mar. Geol. 38, 263–282.

Meyerhof, G.G., 1951. The ultimate bearing capacity of foundations. Geotechnique 1, 301–332.

Meyerhof, G.G., 1976. Bearing capacity and settlement of pile foundations. Proc. ASCE, J. Soil Mech. Found. Div. 102, 197–228.

Montargues, R., Fay, J.-B., Tirant, P.L., 1987. Soil reconnaissance at great water depth. Proceedings 4th International Conference on Deep Offshore Technology.

Montargues, R., Tirant, P.L., Wannesson, J., Valery, P., Berthon, J.-L., 1983. Large-size stationary piston core. Proceedings 2nd International Conferance on Deep Offshore Technology, pp. 63–74.

Moreno, E., Thouveny, N., Delanghe, D., McCave, I.N., Shackleton, N.J., 2002. Climatic and oceanographic changes in the Northeast Atlantic reflected by magnetic properties of sediments deposited on the Portuguese Margin during the last 340 ka. Earth Planet. Sci. Lett. 202, 465–480.

Paik, K., Lee, S., 1993. Behaviour of soil plugs in open-ended model piles driven into sands. Mar. Georesourc. Geotechnol. 11, 353–373.

Parker, W.R., 1991. Quality control in mud coring. Geo-Mar. Lett. 11, 132–137.

Parker, W.R., Sills, G.C., 1990. Observation of corer penetration and sample entry during gravity coring. Mar. Geophys. Res. 12, 101–107.

Poulos, H.G., Davies, E.H., 1974. Elastic Solutions for Soil and Rock Mechanics. Wiley, New York.

Randolph, M.F., Leong, E.C., Houlsby, G.T., 1991. One-dimensional analysis of soil plugs in pipe piles. Geotechnique 41, 587–598.

Ross, D.A., Riedel, W.R., 1967. Comparison of upper parts of some piston cores with simultaneously collected open-barrel cores. Deep-Sea Res. 14, 285–294.

Schilling, J., van Weering, T.C.E., Eisma, D., 1988. Advantages of light-weight Kevlar rope for ocean bottom sampling with piston corer and box corer. Mar. Geol. 70, 149–152.

Shackleton, N.J., Hall, M.A., Vincent, E., 2000. Phase relationships between millennial-scale events 64,000-24,000 years ago. Paleoceanography 15, 565–569.

Shen, C., Hastings, D., Lee, T., Chiu, C.-H.S., Lee, M.-Y., Wei, K.-Y., Edwards, R.L., 2001. High precision glacial-interglacial benthic foraminiferal Sr/Ca records from the eastern equatorial Atlantic Ocean and Caribbean Sea. Earth Planet. Sci. Lett. 190, 197–209.

Silva, A.J., Hollister, C.D., Laine, E.P., Beverly, B.E., 1976. Geotechnical properties of deep sea sediments: Bermuda Rise. Mar. Geotechnol. 1, 195–232.

Silva, A.J., Hollister, C.D., 1979. Geotechnical properties of ocean sediments recovered with the giant piston corer: Blake-Bahama Outer Ridge. Mar. Geol. 29, 1–22.

Smith, G.N., Smith, I.G.N., 1998. Elements of Soil Mechanics, 7th edn. Blackwell Science, London.

Storms, M.A., 1990. Ocean Drilling Program (ODP) Deep Sea Coring Techniques. Mar. Geophys. Res. 12, 109–130.

Thomson, J., Summerhayes, C.P., Schonfeld, J., Zahn, R., Grootes, P., 1999. Implications for sedimentation changes on the Iberian Margin over the last two glacial/interglacial transitions from $^{230}Th_o$ systematics. Earth Planet. Sci. Lett. 165, 170–255.

Thouveny, N., Moreno, E., Delanghe, D., Candon, L., Lancelot, Y., Shackleton, N.J., 2000. Rock magnetic detection of distal ice-rafted debris: clue for the identification of Heinrich layers on the Portuguese Margin. Earth Planet. Sci. Lett. 180, 61–75.

Weaver, P.P.E., Schultheiss, P.J., 1983. Detection of repenetration and sediment disturbance in open-barrel gravity cores. J. Sediment. Petrol. 53, 649–654.

Weaver, P.P.E., Schultheiss, P.J., 1990. Current methods for obtaining, logging and splitting marine sediment cores. Mar. Geophys. Res. 12, 85–100.

Zangger, E., McCave, I.N., 1990. A redesigned kasten core barrel and sampling technique. Mar. Geol. 94, 165–171.